Available online at www.sciencedirect.com
SCIENCE DIRECT®
Carbohydrate Research 340 (2005) 107–113
Carbohydrate RESEARCH

Starch crystal solubility and starch granule gelatinisation

Perrine Crochet, Thierry Beauxis-Lagrave, Timothy R. Noel, Roger Parker* and Stephen G. Ring

Molecular Biophysics Group, Institute of Food Research, Norwich Research Park, Colney Lane, Norwich, NR4 7UA, UK

Received 20 May 2004; received in revised form 20 October 2004; accepted 5 November 2004
Available online 25 November 2004

Abstract—The solubility and dissolution behaviour of A- and B-type crystals of short chain amylose were measured both directly and using differential scanning calorimetry in the temperature range 30–110 °C. Dissolution in the calorimeter was affected by superheating to the extent of 24–28 °C. Following trends previously found by calorimetry the B-type crystal polymorph was more soluble than the A-type. Analysis of the chain composition of the dissolved material revealed a preferential solubilisation of the short chains at the lower temperatures. The solubility of both crystal polymorphs and the magnitude of the preferential solubilisation effect was reduced in the presence of 30% w/w sucrose. A comparison of calorimetric measurements of crystal dissolution and the gelatinisation of native granular waxy maize and potato starches found some broad similarities, such as transition temperatures and their composition dependence, and some differences, such as the relatively narrow temperature range of granular gelatinisation, which reflects its cooperative nature.

Keywords: Starch; Polymorphism; Solubility; Phase diagram; Granules; Gelatinisation

1. Introduction

The semi-crystalline structure of starch is important during its biosynthesis[1] and affects its food[2,3] and nonfood uses.[4] In foods, crystalline structure can be used to control the extent to which starch is digested in the upper gut or fermented in the colon.[2,3] The structural complexity of starch at both the molecular and supramolecular levels means that useful insights into its behaviour can be obtained using simpler model systems. The effects of crystal polymorph,[5] molecular weight,[6–8] chain branching[9] and starch–water interactions[8] on association and dissolution phenomena have been characterised and interpreted at the molecular level by studying the behaviour of isolated amylose and amylopectin, synthetic amyloses and short chain amyloses prepared by acid hydrolysis.

Starch chains crystallise in two polymorphic forms, the A- and B-type structures, which X-ray diffraction and crystal structure modelling studies[10,11] have shown to be based on left-handed double-stranded helices parallel-packed into monoclinic and hexagonal unit cells, respectively. Native starch granules show the same diffraction patterns and crystal structures with cereal starches showing the A-type pattern and tuber starches showing the B-type pattern.[1] Mixtures of A- and B-type, designated C-type also occur, for example in wild type pea starch, in which B-type occurs at the centre of the granule and A-type around the periphery.[12] Calorimetric studies of the melting behaviour of highly crystalline A- and B-type spherulites of short chain amylose show that the A-type melts at higher temperatures than the B-type and that, on reducing the water content, the melting temperature of both polymorphs increases,[5] behaviour typical for a polymer-diluent system.[13] A more recent study using fractions of different chain length[8] shows that, at a volume fraction of 0.2, the melting temperature increases from 58 to 120 °C as the mean degree of polymerisation (DP) increases from 12 to 57, a behaviour predicted theoretically and previously studied in synthetic polymers.[13] While these calorimetric studies have mapped out the phase behaviour, the use of

* Corresponding author. Tel.: +44 01603 255000; fax: +44 01603 507723; e-mail: roger.parker@bbsrc.ac.uk

0008-6215/$ - see front matter © 2004 Elsevier Ltd. All rights reserved.
doi:10.1016/j.carres.2004.11.006

scanning calorimetry with typical scanning rates of 10 °C/min means that the melting temperatures may be affected by kinetic factors. In the present study the phase diagrams of the A- and B-forms of short chain amylose crystals are measured directly by analysis of the composition of saturated solutions, which allows their solubility to be measured over longer time scales than in the previous studies and additionally allows the characterisation of the chain distribution of solubilised material to discover whether any fractions are preferentially solubilised.

Understanding the influence of the amorphous and crystalline structures and the overall granular form of the native starch granule on gelatinisation is a complex problem.[14–19] The complexity means that it is difficult to design critical experiments, which clearly distinguish between different interpretations. Factors to be considered include the water relations both internal and external to the granule,[14–16] the role of the amorphous and crystalline regions of the granule and their interrelationship[14,15,17,20] and the extent to which equilibrium and kinetic factors determine behaviour.[18,19] Differences in interpretation date from the earliest calorimetric studies of starch gelatinisation. Donovan[14] found that, on heating, potato starch–water mixtures show one or two endothermic transitions, the number depending upon the water content. For water contents above 60% w/w only a single, largely temperature-invariant, endothermic transition occurs. On acid treatment, a process, which selectively degrades the amorphous portions of the granule, the transition temperature increased, which was explained in terms of the removal of the swelling stress due to the amorphous regions of the granule.[15] Evans and Haisman[16] criticised this explanation as being unnecessarily complicated, proposing instead that the observation of a single temperature-invariant transition could straightforwardly be explained in terms of the similarly invariant composition of the granule when swollen in pure water. More recently, small angle scattering and related studies have lead to the interpretation of the gelatinisation of starch in terms of consecutive smectic-isotropic and helix-coil transitions of a side-chain liquid crystalline polymer,[17] which has most in common with Donovan's view of gelatinisation in excess water ($\geqslant$60% w/w). Another recurrent argument concerns the extent to which the observed transitions represent equilibrium or kinetic behaviour.[18,19] In the present study we compare the dissolution of short chain amylose crystals with the gelatinisation of native starch granules with the aim of better understanding this problem.

A comprehensive model of the solubility behaviour of starch should include interactions of other components in addition to starch and water. In the present study the effects of sucrose addition on the solubility has been included as a variable. In a previous study of preferential solvent interactions and the dissolution of B-type spherulites it was found that there was no preferential interaction with D-glucose and an elevation of the melting temperature on D-glucose addition.[21] Further interpretation was hampered by the lack of an adequate thermodynamic model of the dissolution process and the question as to what extent the experimental results represented equilibrium behaviour. Here the effects of sucrose addition on crystal dissolution and granule gelatinisation are compared.

2. Materials and methods

2.1. Materials

Waxy maize and potato starches were obtained from Sigma, Poole, Dorset. Hydrochloric acid was from Riedel de Haën, sodium hydroxide and sodium acetate (both electrochemical detection grade) from Fisher Scientific, sucrose from Sigma and ethanol from BDH. All reagents were at least analytical grade. Water was from an Elga Maxima water purification system (Vivendi Water Systems, High Wycombe, Bucks) with a resistivity of 18 MΩ cm.

2.2. Potato starch lintnerisation and crystal preparation

Short starch chains were prepared by prolonged acid hydrolysis of potato starch as described previously.[5] The method is based upon that of Robin et al.[22] Mixtures of 10% w/w starch and 2.2 M HCl were held at 35 °C for 42 days. The starch granules were gently resuspended each day. The mixture was then neutralised with sodium hydroxide and the sediment washed. This was achieved by repeatedly decanting the supernatant, resuspending the sediment in water and then centrifuging the suspension, until the pH of the supernatant was above 6.0. This starch was further purified by dissolution in an autoclave (121 °C for 15 min), filtering the hot (about 60 °C) solution through a glass sinter (40–100 μm pore size) and then crystallisation by adding an equal volume of hot ethanol and holding at 1 °C for 2 days. This material was then air dried at 35 °C and, finally, vacuum dried for storage.

To prepare the B-type crystals a 10% w/w suspension was heated in a screw-topped Pyrex tube at 120 °C for 15 min, the solution cooled and filtered (5 μm Durapore filter) then reheated to 120 °C. This solution was then cooled from 80 to 1 °C at 5 °C/h and the crystal suspension refrigerated after 48 h. The A-type crystals were prepared by a similar procedure except a 17.5% w/w suspension is used and an equal volume of hot ethanol (T_b, 78.5 °C) added prior to the controlled cooling. The crystals were washed to remove dissolved starch and ethanol by repeatedly decanting the supernatant, resuspending in water and centrifugation. This process was judged

complete by the starch concentration in the supernatant being below 0.5 mg/g and the absence of a solvent (ethanol) peak as measured by size exclusion chromatography. The crystals were stored as concentrated pastes for subsequent measurements. The polymorphic form of the crystals were verified by X-ray diffraction as described previously.[5] The dry weight content of crystal pastes was obtained by vacuum drying at 60 °C over phosphorus pentoxide overnight.

2.3. Crystal solubility measurement

To determine crystal solubility mixtures (about 1 g, 15% w/w crystals) were weighed into 1 mL reaction vessels (Supelco) fitted with screw caps and septa protected by a valve (Mininert, Supelco). Temperature control (±0.2 °C) was achieved by holding the reaction vessels in an aluminium block in an oven. Preliminary measurements showed that at 70 °C the solubility required 10 h to reach steady state. The occurrence of chemical degradation at higher temperatures (120 °C) dictated, however, that a shorter time between temperature steps was necessary. An interval of 2 h was chosen. At this interval the solubility was within 96% of its steady state value. The temperature was increased from 30 to 120 °C in 10 °C steps. Overnight samples were kept at constant temperature. Resampling the following morning showed negligible increase in solubility overnight. Every 30 min samples were vortex mixed for 2 min and returned to the oven. The supernatant was sampled using a 25 μL Hamilton syringe.

2.4. Size exclusion chromatography (SEC)

The concentration of short chain amylose in the supernatant was determined using a Dionex HPLC system equipped with a Phenomenex BioSep S-2000 (300 × 7.8 mm) size exclusion chromatography column (Macclesfield, Cheshire, UK) and Shodex refractive index detector. The eluant was water at an elution rate of 1 mL/min. The column was calibrated using fractions of the eluant from a sample of fully solubilised crystals collected over 0.3 min intervals using a Gilson FC 204 fraction collector. These fractions were subsequently analysed using high performance anion-exchange chromatography to obtain the peak DP of the fraction and reinjected on the SEC system to obtain accurate peak retention times. A linear regression of the retention time-DP data yielded the relationship: retention time (minutes) = $10.951–1.506\log_{10}\mathrm{DP}$.

2.5. High performance anion-exchange chromatography with pulsed amperometric detection (HPAEC-PAD)

The chain length distribution was characterised using HPAEC-PAD. A Gilson gradient HPLC system equipped with a Dionex Carbo-Pac PA-100 (250 × 4 mm) ion exchange column, eluant degas module and pulsed amperometric detector (PAD-2) was used. The eluants were 100 mM sodium hydroxide (A) and 100 mM sodium hydroxide containing 1.0 M sodium acetate (B) and a gradient of 11–36% B over 66 min. The detector pulse potentials and durations were as follows: $E_1 = 0.05$ V, 420 ms; $E_2 = 0.8$ V, 180 ms; $E_3 = -0.15$ V, 360 ms. The sensitivity of the detector was set at 1 kn A. Sample volumes of 20 μL (about 1 mg/g) were loaded onto the column each containing a maltoheptaose internal standard. Peak heights were measured from a linear baseline interpolated between (i) the section of baseline between the DP10 and DP11 peaks and (ii) the baseline at retention times $\geqslant$55 min, a time at which all the samples had eluted.

2.6. Differential scanning calorimetry

Apparent heat capacity changes during crystal dissolution and starch gelatinisation were measured using a Perkin–Elmer DSC 7 differential scanning calorimeter for a starch concentration of 15% w/w at a scanning rate of 10 °C/min. The temperature scale was calibrated using indium (T_m, 156.6 °C) and artificial sapphire was used as the reference material for heat capacity determination. The samples were contained in stainless steel high pressure capsules to allow measurements to be made at temperatures close to the boiling point without capsule leakage. The manufacturers' software was used to calculate the heat capacity and integrate the peaks. The onset and end temperatures of the gelatinisation peaks were determined by the intersection of tangents fitted to the leading and trailing flanks of the peak with the baseline.

3. Results

The elution profile from the HPAEC of the fully solubilised A-type crystals is shown in Figure 1. The elution profile is similar to that obtained elsewhere for extensively lintnerised potato starch with a major fraction centred around DP15 and a second overlapping subfraction centred around DP25. Using enzymatic methods and gel permeation chromatography Robin et al.[22] showed that while the DP15 fraction is primarily linear, the DP25 sub-fraction is singly branched. The low DP cut-off of the chain distribution in Figure 1 is at about DP8-9, which is slightly higher than the co-crystallisation limit of DP6 reported by Gidley and Bulpin.[7] This discrepancy may be due to these fractions being soluble in cold water and being removed during the washing of our crystals. While the HPAEC is able to resolve the peaks of the different chain length fractions, baseline separation is only achieved up to about DP11. For this reason the ratio of the peak heights DP25/DP15 was

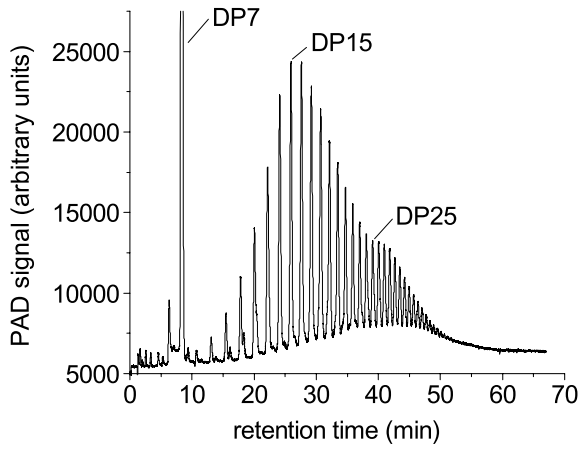

Figure 1. The HPAEC elution profile of the short chain amylose of the A-type crystals showing the chain length distribution. The DP7 peak is the maltoheptaose internal standard.

used to characterise the chain distribution, with a value of 0.38 for the A-type crystals. The elution profile of the fully solubilised B-type crystals (results not shown) showed insignificant differences and the same DP25/DP15 peak height ratio.

The solubility of the A- and B-type crystals in water and 30% w/w sucrose is shown in Figure 2. The crystals have a small but measurable solubility at temperatures close to ambient, which shows a progressive increase with increasing temperature until reaching a linear portion at temperatures above 50 °C for the B-type crystals and above 60 °C for the A-type crystals. Throughout the temperature range the B-type crystals are more soluble than the A-type as observed in earlier calorimetric studies[5] and the slope of the B-type solubility curve is greater. This confirms the B-type crystal polymorph as a metastable kinetic product.[5] This is analogous to the behaviour of triglycerides for which rapid cooling to

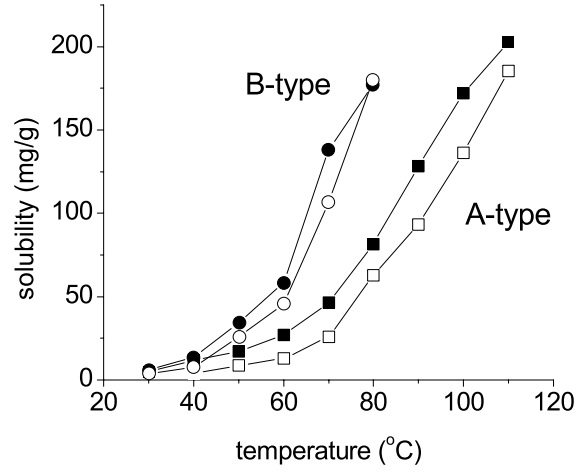

Figure 2. Solubility of the A- and B-type crystals in water (■, ●) and 30% w/w sucrose (□, ○).

Table 1. Chain distribution of amylose dissolved from crystals as indicated by DP25/DP15 peak height ratios measured using HPAEC-PAD

Temperature (°C)	A-type in water	A-type in 30% w/w sucrose	B-type in water	B-type in 30% w/w sucrose
30	0.14	0.21	0.16	0.21
60	0.14	0.18	0.28	0.26
90	0.31	0.32	0.41	0.41
120*	0.27	0.29	0.29	0.17

* At 120 °C degradation is occurring.

low temperatures results in the formation of a metastable, lower density α-phase rather than the equilibrium β-phase.[23,24] At temperatures above 110 °C degradation occurred as indicated by high DP material (⩾DP25) disappearing and shorter chain fractions (>DP10) appearing in the HPAEC results. This places an upper limit on the temperatures at which solubility may be measured by this method. The presence of sucrose reduced the solubility throughout the temperature range by typically 10–35 mg/g, an amount, which is relatively small compared with the sucrose concentration of 300 mg/g.

The HPAEC characterised the amylose chain distribution in solution for the different crystal polymorphs and solution conditions. At the lowest temperatures (30 and 60 °C) the DP25/DP15 peak height ratio (Table 1) are well below the ratio for the fully solubilised crystals (0.38) indicating that the shorter chains are preferentially solubilised at these temperatures. At higher temperature (90 °C) the ratio increases indicating that the longer chains are solubilised, reaching the maximum value for the fully solubilised B-type crystals. The reduction in the peak height ratio at 120 °C indicates the occurrence of chain degradation after prolonged heating. In the presence of 30% w/w sucrose the ratios indicate less preferential solubilisation of the shorter chains at the lowest temperatures. The SEC peak profiles confirmed the occurrence of the preferential solubilisation. Figure 3 shows the effect of dissolution temperature on the normalised peak profiles for solutions saturated with the A-type crystals. Whereas at the lowest temperatures (30 and 50 °C) there is a single symmetrical peak due to the fraction centred about DP15, as the temperature increases above 70 °C, a shoulder appears on the peak at shorter retention times, corresponding to the solubilisation of higher molecular weight fractions. The observation of preferential solubilisation is consistent with the previous calorimetric studies on the melting of short-chain amyloses with narrow molecular weight ranges, which showed that the peak melting temperature of 23.3% w/w mixtures increased from 67 to 102 °C as the DP increased from 15 to 25,[8] that is, with increasing molecular weight the crystals decrease in solubility.

The apparent heat capacity (Fig. 4) of the crystals show broad endotherms during dissolution in the differ-

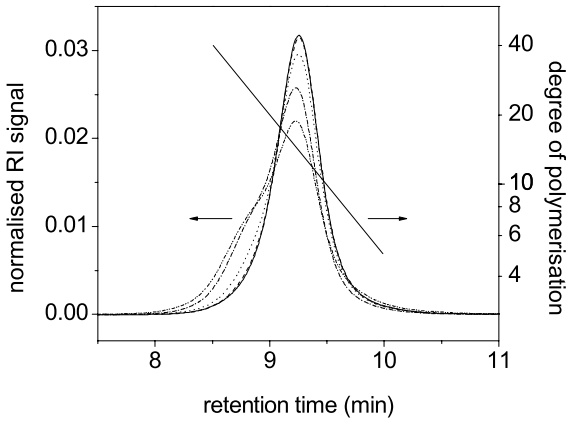

Figure 3. Normalised SEC peak profile for the short chain amylose dissolved from A-type crystals at a range of temperatures: 30 °C, solid line; 50 °C, dashed line; 70 °C, dotted line; 90 °C, dot–dash line; 110 °C, dot–dot–dash line.

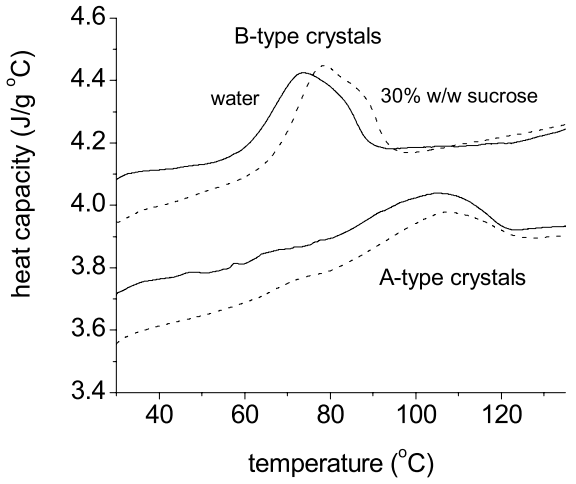

Figure 4. The apparent heat capacity as 15% w/w A- and B-type crystals dissolve in water (—) and 30% w/w sucrose (----). Data has been shifted vertically to aid clarity.

ential scanning calorimeter. Temperatures characterising the endothermic peaks are tabulated in Table 2. The peak temperature of the endotherm for the B-type crystals is about 30 °C below that of the A-type. The A-type endotherm is relatively broad and unsymmetrical, the endothermic heat flow increasing over an interval of 50 °C prior to reaching its peak. The peaks are broader by 10–15 °C than obtained previously,[5] which

Table 2. Effect of polymorphic form and solvent on the temperatures characterising the DSC endotherm during the dissolution of crystals

Sample	T_{onset} (°C)	T_{peak} (°C)	T_{end} (°C)
A-type in water	54 ± 1	104 ± 2	121 ± 2
A-type in 30% w/w sucrose	65 ± 0.3	107 ± 2	131 ± 2
B-type in water	50 ± 1	75 ± 1	97 ± 1
B-type in 30% w/w sucrose	51 ± 0.5	79 ± 0.5	103 ± 3

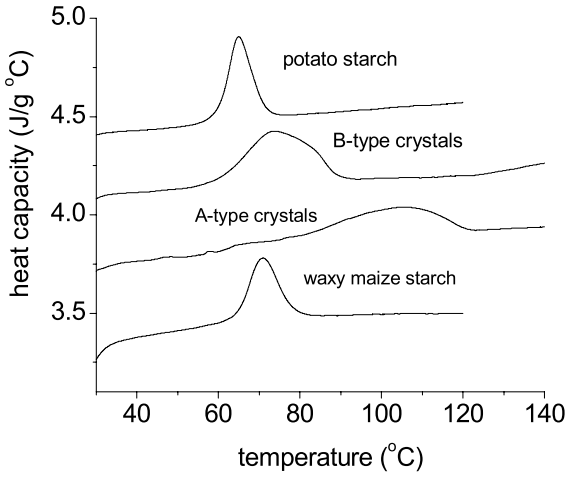

Figure 5. The apparent heat capacity as A- and B-type crystals dissolve in water and potato and waxy maize starch are gelatinised at 15% w/w. Data has been shifted vertically to aid clarity.

Table 3. Effect of botanical source and solvent on the temperatures characterising the DSC endotherm during the gelatinisation of starch granules

Sample	T_{onset} (°C)	T_{peak} (°C)	T_{end} (°C)
Waxy maize in water	65.2 ± 0.6	70.6 ± 0.2	77.1 ± 0.6
Waxy maize in 30% w/w sucrose	74.6 ± 0.3	80.6 ± 0.4	89.1 ± 0.3
Potato in water	60.6 ± 0.6	65.3 ± 0.4	72.3 ± 0.5
Potato in 30% w/w sucrose	70.9 ± 0.3	76.2 ± 0.5	82.2 ± 0.5

we believe to be due a longer crystallisation leading to more heterogeneous crystal dispersion. In the presence of sucrose the endotherms show a shift to higher temperature of about 3–4 °C.

The calorimetric behaviour of the A- and B-type crystals in water is compared with that of native waxy maize and potato starch in Figure 5. The gelatinisation endotherms are relatively narrow (spanning about 25 °C) and symmetrical compared with the behaviour of the crystals (see Table 3 for temperatures characterising peaks). Comparing the peak temperatures of the endotherm of the starches with the corresponding crystals shows that the granule transitions are at temperatures 33 and 10 °C lower for A- and B-type, respectively. In the presence of sucrose the starch granule endotherm peak temperatures increase by about 10 °C (see Table 3) as shown for waxy maize starch in Figure 6.

4. Discussion

4.1. Comparison of crystals' behaviour in solubility experiment and DSC

The crystal dissolution as measured in the solubility experiment and the DSC are most readily compared

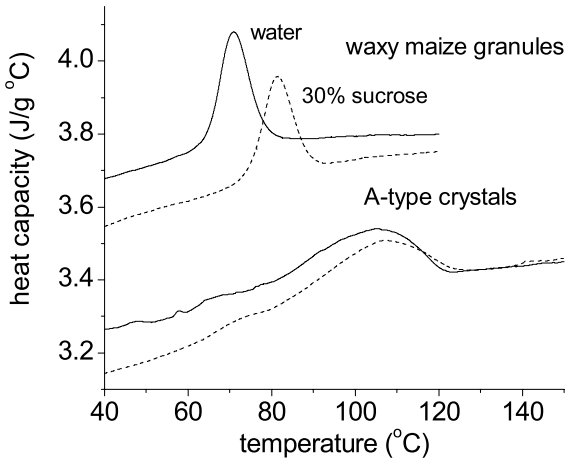

Figure 6. The apparent heat capacity of 15% w/w A-type crystal dissolution and waxy maize gelatinisation in water (—) and 30% w/w sucrose (----). Data has been shifted vertically to aid clarity.

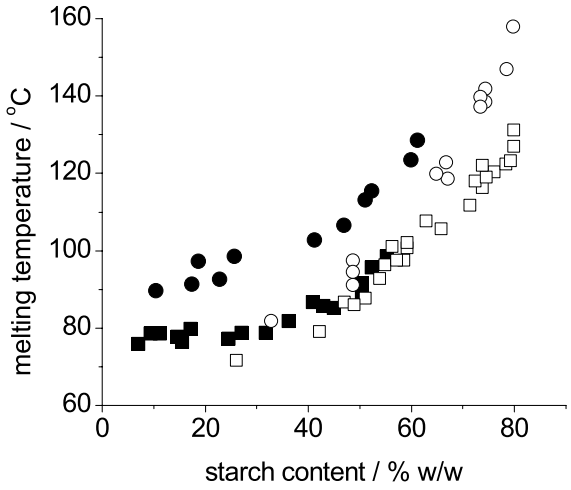

Figure 7. A comparison of the effect of water content on the melting temperatures of A- and B-type spherulites (●, ■, respectively),[5] waxy maize starch (○)[25] and potato starch (□).[14]

by determining the temperature at which dissolution is complete for a particular solute concentration. These temperatures are interpolated from the phase diagram (Fig. 2) at a concentration of 15% w/w (the concentration in the DSC pan) as 73, 76, 95 and 103 °C for the B-type crystals in water, B-type crystals in 30% w/w sucrose, A-type crystals in water and A-type crystals in 30% w/w sucrose, respectively. Comparison of these temperatures with the DSC endotherm end temperature (T_{end}) in Table 2 indicates that the material is dissolving at temperatures, which are 24–28 °C higher in the calorimeter. This indicates that nonequilibrium effects such as superheating and diffusion limitation are occurring in the calorimeter. The two techniques differ in terms of overall heating rates by a factor of 120, the scanning rate of the calorimeter is 10 °C/min whereas in the solubility experiment the sample was heated 10 °C/2 h. The stirring in the solubility experiment also aids equilibration as the convection removes dissolving material from the vicinity of the crystal–solution interface whereas in the calorimeter mass transfer is solely by diffusion. We conclude that while the two techniques are probing the same process the scanning rates in the DSC mean that the results for these crystal dispersions are to some extent nonequilibrium.

4.2. Comparison of the DSC behaviour of crystals and native starches

Before discussing the present results comparing the DSC behaviour of crystals and starch granules we briefly review previous work. Figure 7 collects together previous studies on the effect of water on the melting temperatures of A- and B-type spherulites[5] and the gelatinisation of waxy maize[25] and potato starch.[14] For the starch granules a single point is plotted for the excess water gelatinisation peak and the other points, at higher starch contents, are the higher temperature endothermic melting peaks. Particularly in the region of overlap of the B-type spherulite and the potato starch granule data points (26% w/w to 52% w/w starch) the similarity in transition temperatures and their dependence on water content must originate from the two processes of spherulite dissolution and granule gelatinisation having a common origin. By this argument we deduce that, at least over this water content range, the amorphous parts of the granule are exerting little influence on the gelatinisation processes and the processes is, to a large extent, a thermodynamically-controlled dissolution process.

In contrast, when results at higher water content are examined in detail, it can be seen that there are significant differences (Fig. 5). For example, comparing the results of potato starch gelatinisation with B-type spherulite dissolution it is found that the spherulites dissolve at higher temperatures and over a wider temperature range. The shift to higher temperatures can most simply be explained in terms of the crystals having a higher molecular weight and greater perfection in the absence of the constraints of amylopectin chain branching in the native granule. The differences in the range of temperatures over which the dissolution process occurs reflects the cooperative nature of granule gelatinisation. The arguments of Evans and Haisman[16] are sufficient to explain this phenomenon. When the separate helix-forming chains of the crystal dissolve they are free to distribute themselves throughout the solution. In contrast, within the granule, each amylopectin molecule is involved in many different crystals and once a particular chain is in a coiled conformation it will hydrate to the extent allowed by the overall swelling of the intra-granular network. On this transition from crystalline/double helical to coiled conformation the chain swaps from contributing to the crosslinking of the granule to con-

tributing to its swelling. Assuming that increased intragranular water content allows further dissolution this mechanism would lead to the narrow cooperative gelatinisation peak of the starch granule.

The presence of 30% w/w sucrose elevates both the peak temperature of granular gelatinisation and crystal melting (Fig. 6, Tables 2 and 3). From the calorimetry and the crystal phase diagram (Fig. 2) it is clear that the 30% w/w sucrose–water is a less good solvent for the starch than water. While the larger magnitude of the temperature elevation of the granular starch may require further explanation we take these observations as further evidence that gelatinisation is to a large extent a thermodynamically-controlled dissolution process.

5. Conclusions

Using direct analysis of the compositions of solutions saturated with short-chain amylose crystals their equilibrium solubilities have been measured. This technique provides unambiguous information on the effects of different solvents and solution conditions on the solubility of starch chains. In agreement with the previous calorimetric measurements, the A-type crystals were found to be less soluble than the B-type and, as indicated by preferential solubilisation, the solubility decreased with increasing chain length. While the phase diagram describing the dissolution of the crystals and the gelatinisation of granular starch show similarities in terms of transition temperatures and composition dependence, a detailed comparison in the two processes showed both differences in terms of temperature and, probably the distinctive characteristic of granule gelatinisation, its highly cooperative nature. While granular gelatinisation has aspects related to connectivity of the crystallites through the amylopectin chains and the overall granular form, it can also be related to the thermodynamic behaviour of related model systems.

Acknowledgements

T.R.N., R.P. and S.G.R. thank the BBSRC for financial support through the Core Strategic Grant. T.B.-L. and P.C. acknowledge the support of the EU through the Leonardo scheme.

References

1. Buleon, A.; Colonna, P.; Planchot, V.; Ball, S. *Int. J. Biol. Macromol.* **1998**, *23*, 85–112.
2. Pohu, A.; Putaux, J. L.; Planchot, V.; Colonna, P.; Buleon, A. *Biomacromolecules* **2004**, *5*, 119–125.
3. Leloup, V. M.; Colonna, P.; Ring, S. G. *J. Cereal Sci.* **1992**, *16*, 253–266.
4. van Soest, J. J. G.; Vliegenthart, J. F. G. *Trends Biotechnol.* **1997**, *15*, 208–213.
5. Whittam, M. A.; Noel, T. R.; Ring, S. G. *Int. J. Biol. Macromol.* **1990**, *12*, 359–362.
6. Gidley, M. J.; Bulpin, P. V. *Macromolecules* **1989**, *22*, 341–346.
7. Gidley, M. J.; Bulpin, P. V. *Carbohydr. Res.* **1987**, *161*, 291–300.
8. Moates, G. K.; Noel, T. R.; Parker, R.; Ring, S. G. *Carbohydr. Res.* **1997**, *298*, 327–333.
9. Orford, P. D.; Ring, S. G.; Carroll, V.; Miles, M. J.; Morris, V. J. *J. Sci. Food Agric.* **1987**, *39*, 169–177.
10. Imberty, A.; Perez, S. *Biopolymers* **1988**, *27*, 1205–1221.
11. Imberty, A.; Chanzy, H.; Perez, S.; Buleon, A.; Tran, V. *J. Mol. Biol.* **1988**, *201*, 365–378.
12. Bogracheva, T. Y.; Morris, V. J.; Ring, S. G.; Hedley, C. L. *Biopolymers* **1998**, *45*, 323–332.
13. Prasad, A.; Mandelkern, L. *Macromolecules* **1989**, *22*, 914–920.
14. Donovan, J. W. *Biopolymers* **1979**, *18*, 263–275.
15. Donovan, J. W.; Mapes, C. J. *Starch* **1980**, *32*, 190–193.
16. Evans, I. D.; Haisman, D. R. *Starch* **1982**, *34*, 224–231.
17. Waigh, T. A.; Gidley, M. J.; Komanshek, B. U.; Donald, A. M. *Carbohydr. Res.* **2000**, *328*, 165–176.
18. Perry, P. A.; Donald, A. M. *Carbohydr. Polym.* **2002**, *49*, 155–165.
19. Perry, P. A.; Donald, A. M. *Biomacromolecules* **2000**, *1*, 424–432.
20. Jenkins, P. J.; Donald, A. M. *Carbohydr. Res.* **1998**, *308*, 133–147.
21. Moates, G. K.; Parker, R.; Ring, S. G. *Carbohydr. Res.* **1998**, *313*, 225–234.
22. Robin, J. P.; Mercier, C.; Charbonniere, R.; Guilbot, A. *Cereal Chem.* **1974**, *51*, 389–406.
23. Gidley, M. J. *Carbohydr. Res.* **1987**, *161*, 301–304.
24. Small, D. M. *Handbook of Lipid Research, Volume 4, The Physical Chemistry of Lipids. From Alkanes to Phospholipids*; Plenum: New York, 1986, pp 362–367.
25. Russell, P. L. *J. Cereal Sci.* **1987**, *6*, 133–145.